# Reduced cardiolipin content decreases respiratory chain capacities and increases ATP synthesis yield in the human HepaRG cells

Laure Peyta, Kathleen Jarnouen, Michelle Pinault, Cyrille Guimaraes, Jean-Paul Pais de Barros, Stephan Chevalier, Jean-François Dumas, François Maillot, Grant M. Hatch, Pascal Loyer, et al.

# Reduced cardiolipin content decreases respiratory chain capacities and increases ATP synthesis yield in the human HepaRG cells

Laure Peyta[1], Kathleen Jarnouen[2,3], Michelle Pinault [1], Cyrille Guimaraes[1], Jean-Paul Pais de Barros[4], Stephan Chevalier[1], Jean-François Dumas[1], François Maillot[1,5], Grant M. Hatch[6], Pascal Loyer[2,3] and Stephane Servais[1].

[1] Inserm UMR1069, *Nutrition, Croissance et Cancer*, Université François Rabelais de Tours- 10, bd Tonnellé - 37032 Tours Cedex, France. *laure.peyta@etu.univ-tours.fr; michelle.pinault@univ-tours.fr; cyrille.guimaraes@gmail.com; stephan.chevalier@univ-tours.fr; jean-francois.dumas@univ-tours.fr; maillot@med.univ-tours.fr; stephane.servais@univ-tours.fr*

[2] Inserm UMR S-991, *Foie, Métabolismes et Cancer*, CHU Pontchaillou, 2 rue Henri Le Guilloux, 35033 Rennes, France. *kathleen.jarnouen@univ-rennes1.fr; pascal.loyer@univ-rennes1.fr*

[3] Université de Rennes 1, 2 rue du Thabor CS46510, 35065 Rennes cedex France

[4] Plateforme de Lipidomique. INSERM UMR866 / LabEx LipSTIC, 15 Bd Mal de Lattre de Tassigny, 21000 Dijon, France. *jppais@u-bourgogne.fr*

[5]CHRU de Tours, Département de Médecine Interne, 2, boulevard Tonnellé - 37044 Tours cedex 9, France.

[6] Department of Pharmacology and Therapeutics, Biochemistry and Medical Genetics, Faculty of Health Sciences, Center for Research and Treatment of Atherosclerosis, DREAM Children's Hospital Research Institute of Manitoba, University of Manitoba, 513 – 715 McDermot Avenue Winnipeg MB R3E 3P4, Manitoba, Canada. *ghatch@chrim.ca*

Corresponding author:

Stephane SERVAIS, Laboratoire Nutrition, Croissance et Cancer - Inserm UMR1069

Faculté de Médecine - 10, bd Tonnellé - 37032 Tours Cedex

Email stephane.servais@univ-tours.fr; Phone +33 2.47.36.60.59; Fax +33 2 47 36 62 26

**Abstract**

Cardiolipin (CL) is a unique mitochondrial phospholipid potentially affecting many aspects of mitochondrial function/processes, i.e. energy production through oxidative phosphorylation. Most data focusing on implication of CL content and mitochondrial bioenergetics were performed in yeast or in cellular models of Barth syndrome. Previous work reported that increase in CL content leads to decrease in liver mitochondrial ATP synthesis yield. Therefore the aim of this study was to determine the effects of moderate decrease in CL content on mitochondrial bioenergetics in human hepatocytes. For this purpose, we generated a cardiolipin synthase knockdown (shCLS) in HepaRG hepatoma cells showing bioenergetics features similar to primary human hepatocytes. shCLS cells exhibited a 55% reduction in CLS gene and a 40% decrease in protein expression resulting in a 45% lower content in CL compared to control (shCTL) cells. Oxygen consumption was significantly reduced in shCLS cells compared to shCTL regardless of substrate used and energy state analyzed. Mitochondrial low molecular weight supercomplexes content was higher in shCLS cells (+60%) compared to shCTL. Significant fragmentation of the mitochondrial network was observed in shCLS cells compared to shCTL cells. Surprisingly, mitochondrial ATP synthesis was unchanged in shCLS compared to shCTL cells but exhibited a higher ATP:O ratio (+46%) in shCLS cells. Our results suggest that lowered respiratory chain activity induced by moderate reduction in CL content may be due to both destabilization of supercomplexes and mitochondrial network fragmentation. In addition, CL content may regulate mitochondrial ATP synthesis yield.

Highlights:

- First validation of HepaRG hepatocyte-like cells as a new alternative model for bioenergetics studies in human hepatocytes.
- First data in human hepatocyte cell lines demonstrating that moderate reduction in cardiolipin content reduced mitochondrial oxidative capacities.
- Cardiolipin content is part of the regulation of ATP synthesis yield since reduction in cardiolipin content increases ATP synthesis yield.

Key words: cardiolipin synthase, mitochondrial network, supercomplexes, oxidative phosphorylation, hepatocytes

## Introduction

Cardiolipin (CL) is a unique phospholipid because of i) its chemical structure consisting of two phosphate headgroups, which are attached by a glycerol moiety, and four acyl chains providing large diversity in CL molecular species; ii) its specific location in mitochondrial membranes, which is also its synthesis site; iii) its interactions with numerous mitochondrial proteins, including oxidative phosphorylation complexes, positioning it in many aspects of mitochondrial function/processes, including energy production through oxidative phosphorylation [1], stabilization of supercomplexes [2,3], mitochondrial fission and fusion [4], protein import [5], mitophagy [6–8] and mitochondria-mediated apoptosis [9,10]. CL effects on respiratory complexes activity has been shown *in silico*. CL binds to complex I [11–13], II [14], III [11,15,16] and IV [17–19] and ensures their optimal activities. In *in vitro/in vivo* experiments, most knowledge of CL role in these fundamental functions of mitochondria comes from studies in the yeast *Saccharomyces cerevisiae*. Contrary to higher Eukaryotes [20], yeast are viable in the absence of CL. For example, the Δcrd1 mutant has been extensively used [1,21–24]. Although useful for studying mechanisms of CL metabolism and function yeast models may have limited applicability to the mammalian system. In fact, in this unicellular eukaryotic cell the composition of the mitochondrial respiratory chain is markedly different between mammals since complex I is absent. However supercomplexes, although different in composition, are conserved between yeast and mammals.

Few rigorous studies have examined mitochondrial bioenergetics modulated through an increase or a reduction in CL content in mammalian cells. A Chinese hamster ovary (CHO) cell line containing a temperature-sensitive mutant of PG synthase provided the first indication of CL involvement in mitochondrial bioenergetics in mammalian cells [25]. In alpha-synuclein knockout mice, brain CL content was lowered in relation to a reduction in respiratory complex I/III activity [26]. Protein Tyrosine Phosphatase localized to the Mitochondrion 1 (PTPMT1)

deficient mouse embryonic fibroblasts exhibited a 3.5-fold reduction in CL content and this was associated with a reduction in oxygen consumption in all energy states [20]. Others studies in mammals cells have used knockdown of cardiolipin synthase (CLS), the specific enzyme of *de novo* CL synthesis [24], but with a focus on apoptosis and not mitochondrial bioenergetics [9,27]. The role of CL in mitochondrial bioenergetics has been examined in cellular or animal models of Barth syndrome. These models are characterized by not only a reduction in CL content but an accumulation in monolysocardiolipin (MLCL). Therefore, the alterations in mitochondrial bioenergetics reported in Barth syndrome models may not be exclusively due to reduced CL content. In addition, the mitochondrial alterations in Barth syndrome are subject to debate [28,29]. Other studies have evaluated the effect of CL enrichment on mitochondrial bioenergetics. Direct addition of CL to an oxygraphy chamber induced an increase in oxygen consumption in non-phosphorylating and phosphorylating states in isolated liver mitochondria [30]. Our group further confirmed these effects with the demonstration that the increase in liver mitochondria CL content was associated with a specific increase in energy wasting (in non-phosphorylating state) and a reduction in ATP synthesis yield [31].

Since there is no data that has clearly examined the effect of CL reduction on mitochondrial bioenergetics in human cells and that CL content can modulate ATP synthesis yield, the aim of the present study was to determine the effects of a partial decrease in CL content on mitochondrial bioenergetics in human hepatocytes.

## Material and methods

### *Cell culture*

As previously described [32], HepaRG cells (obtained from Biopredic International, France) were cultivated in William's E medium supplemented with 10% fetal bovine serum, 100 U/ml penicillin, 100 µg/ml streptomycin, 5 µg/ml insulin, and 50 µM hydrocortisone hemisuccinate. After 2 weeks, the medium was supplemented with 2% dimethyl sulfoxide (DMSO) and the cells were cultured for 2 more weeks. HepaRG hepatocytic cells from DMSO treated cultures were selectively detached using gentle trypsination for experiment use. HepG2 cells (ATCC, USA) were cultivated in MEM medium supplemented with 10% fetal bovine serum, 100 U/ml penicillin, 100 µg/ml streptomycin, 2 mM L-glutamine and 1% non-essential amino acids. Huh7 cells (ATCC, USA) were cultivated in DMEM medium supplemented with 10% fetal bovine serum, 100 U/ml penicillin, 100 µg/ml streptomycin and 2 mM L-glutamine.

Human primary hepatocytes were obtained from the processing of biological samples through the Centre de Ressources Biologiques (CRB) Santé of Rennes BB-0033-00056. The research protocol was conducted under French legal guidelines and fulfilled the requirements of the local institutional ethics committee. Hepatocytes were isolated from partial liver resections by a two-step collagenase perfusion procedure. Liver parenchymal cells were seeded at a density of 1.5 x $10^5$ viable cells/$cm^2$ dish in Williams E medium supplemented with 0.2% bovine serum albumin, 0.01% insulin, 2 mM of l-glutamine, 100 U/ml of penicillin, 10 µg/ml of streptomycin, 0.1 µM hydrocortisone hemisuccinate and 10% FCS. Twenty four hours after plating, the primary human hepatocytes were cultured in the William's E medium supplemented with 2% DMSO used for the differentiated HepaRG cells. The medium was renewed daily and hepatocytes were used for experiments 2 to 4 days after plating.

### *Generation of CLS Knockdown Cells*

CLS shRNA and non-silencing negative control pGIPZ lentiviral particles were purchased from Thermo Scientific (Fermentas, Gmbh, Sankt Leon-Rot, Germany). Three pGIPZ viral particles (source clone identifications: V3LHS_414357, V2LHS_176631, V2LHS_176630) encoding shRNA targeting CLS gene (Fermentas nomenclature: CLRS1) were tested. In our culture conditions, the most efficient repression of CLS expression was obtained using the V2LHS_176630 viral particles (data not shown), which was kept for the large scale production of stable recombinant HepaRG cells. Viral titer of CLS and non-silencing pGIPZ lentiviral particles was ~1.2 x $10^8$ Titration Units/mL. For transduction of proliferating HepaRG cells, $10^5$ cells/well in 24-well plates were seeded 24h prior infection, which was performed with the multiplicity of infection at 5 in the absence of polybrene for 48h. The pGIPZ lentiviral vector contains the human cytomegalovirus promoter driving the transgene expression. The transgene includes the turboGreen fluorescent protein (tGFP), an internal ribosome entry site (IRES) followed by the puromycine selection cDNA and the microRNA-adapted shRNA for gene knockdown. One week after infection, the cells were plated in a 60 mm dish and expanded in presence of 250 µg/mL of puromycin. Following cell expansion, ~$5.10^6$ cells were subjected to cell sorting for enrichment of GFP+ cells and selection of cells expressing shRNA. This procedure ensured >80% of $GFP^+$ HepaRG cells.

***RNA isolation and real time PCR assay***

Total RNA from HepaRG cells were extracted with NucleoSpin® RNA II (Macherey-Nagel) following manufacturer's instructions. Reverse transcription was performed using High capacity cDNA reverse transcription kit (Applied Biosystems). The Real-time PCR was performed with the StepOnePlus™ System and with the Taqman probe-based assays (Applied Biosystems). Human Taqman primers for CLS (Hs00219512_m1) and the housekeeping gene TBP (TATA binding protein) (Hs00427620_m1) were provided by Applied Biosystems.

***Western blotting***

After boiling in Laemmli buffer (20 mM Tris pH 6.8, 2 M β-Mercaptoethanol, SDS 9%, glycerol 30%), total proteins extract (excepted for DRP1 where mitochondrial proteins were used) were resolved by SDS-PAGE, transferred to polyvinylidenefluoride membrane, blocked in 5% non-fat milk in phosphate-buffered saline (PBS)/Tween-20, blotted and developed with antibodies specific for CLS (14845-1-AP, Proteintech, Manchester, UK), complex I (Grim 19)( ab110240, Abcam), complex II anti SDHA (ab14715, Abcam), complex III UQCRFS1 (ab14746, Abcam), complex IV anti MTCO1 (ab14705), ATP synthase anti ATP5A (ab14748, Abcam), PGC-1α (ab77210, Abcam), mtTFA (ab119684, Abcam), Mitofusin 2 (ab101055, Abcam), DRP1 (ab56788), β adaptin (sct-58226, Santa Cruz Biotechnology) and Voltage Dependent anion channels (VDAC) (ab14734, Abcam) (loading control) followed by horseradish peroxidase-coupled detection (Pierce ECL Western Blotting Substrate). Secondary antibodies were obtained from SantaCruz. The protein band intensities were analyzed by densitometry (MF-ChemiBIS 3.2, DNR Bioimaging Systems, MultiGauge software, Fujifilm).

***Phospholipid classes quantitation***

Mitochondria were extracted from HepaRG cells by differential centrifugation. Then mitochondrial lipids were extracted following the protocol of Bligh and Dyer [33]. In order to quantify mitochondrial phospholipids (cardiolipin [CL], phosphatidylethanolamine [PE], phosphatidylinositol [PI], phosphatidylcholine [PC], phosphatidylserine [PS] and sphingomyelin [SM]), standards and samples were loaded on silica plates using Linomat V sample applicator (CAMAG, Muttenz Switzerland). After migration, the plates were immersed into the following solution (10% wt/vol) copper sulfate in 8% (vol/vol) phosphoric acid solution and then heated at 160°C for 15 min to stain all of the phospholipids. Quantification was performed using Thin

Layer Chromatography-visualizer Reprostar 3® and WinCats VideoScan® software (CAMAG, Muttenz Switzerland). Results were expressed in percent of total mitochondrial phospholipids.

***CL fatty acid molecular species Analysis by LC-MS/MS***

Lipids were extracted from 6 to 8x $10^6$ cells according to the method of Folch *et al*.[34]. In brief, cells were spiked with $(14:0)_4$-CL used as internal standard (250 ng, Avanti Polar Lipids, Coger, Paris, France). Lipids were extracted with 1 ml of saline and 3.5 ml of $CHCl_3$/MeOH (2/1) for 10 min followed by addition of 1.25 ml $CHCl_3$ for 10 min and finally 1.25 ml of distilled water for 5 min. Organic phase was collected and dried under vacuum. Lipid extracts were further solubilized in 100 µl of $CHCl_3$/MeOH /H2O (60/30/4.5) and LC-MS/MS analysis of cardiolipins was conducted as previously described [35].

***High-resolution respirometry***

High resolution respirometry was performed using a 2-ml chamber OROBOROS® Oxygraph 2K (Oroboros Instruments, Innsbruck, Austria) at 37°C. Respiration rates were calculated as the time derivative of oxygen concentration measured in the closed respirometer and expressed per million viable cells and corrected by non-mitochondrial oxygen consumption measured with antimycin A 2 µM. Cells were permeabilized with digitonin (11 µg per $10^6$ cells for HepaRG cell line and human primary hepatocytes, and 8 µg per $10^6$ cells for Huh7 and HepG2 cell lines). Permeabilized cells ($0.5 \times 10^6$ cells mL) were analyzed in respiration buffer medium (10 mM $KH_2PO_4$, 300 mM mannitol, 10 mM KCl, 5 mM $MgCl_2$, 1 mM EGTA and 1 mg/ml BSA fatty acid free). Oxygen consumption was measured at state 3 or phosphorylating state with 1.5 mM ADP, at state 4 or non-phosphorylating state using oligomycin 8 µg/ml and ETS (Electron Transfert System) capacity (maximum uncoupled respiration) induced by Carbonyl cyanide-4-(trifluoromethoxy)phenylhydrazone (FCCP, 0.8 mM). Experiments were carried out with various

combination of substrate: pyruvate and malate (5 mM), succinate (10 mM), or trimethyl pentanediol (TMPD) and ascorbate (400 µM and 5 mM respectively).

***Efficiency of ATP synthesis by mitochondria***

The kinetic response of oxygen consumption and ATP synthesis was determined at 37°C in a respiratory reaction medium (10 mM $KH_2PO_4$, 300 mM mannitol, 10 mM KCl, 5 mM $MgCl_2$, 1 mM EGTA) supplemented with 0.3% (w/v) fatty acid free BSA. The experimental conditions were: permeabilized cells ($0.5 \times 10^6$ cells.ml$^{-1}$), succinate (10 mM), sodium iodoacetate (2 mM) and ADP (1.5 mM). Concomitantly to oxygen consumption measured by OROBOROS® Oxygraph 2K (Oroboros Instruments, Innsbruck, Austria), 10 µl of cell suspension were sampled every minutes over 6 minutes. Reactions were stopped by adding 10 µl of a solution containing 10% perchloric acid and EDTA (25 mM) and then neutralized in a buffer (Hepes 25 mM, EDTA 2 mM, pH 7.75). In order to quantify mitochondrial ATP synthesis, standard ATP solutions from $10^{-11}$ to $10^{-7}$ M and samples were quantified using Enliten ATP assay (Promega) kit and Promega Glomax 20/20 luminometer (Promega). Results were expressed as mg ATP / pmol oxygen.

***Clear Native Electophoresis (CN-PAGE)***

For CN-PAGE, mitochondria were extracted from HepaRG cells by differential centrifugation and were then solubilized in digitonin (5%) dissolved into extraction buffer (Hepes 30 mM, potassium acetate 150 mM, glycerol 12% 6-aminocaproic acid 2 mM and protease inhibitor cocktail) , and the complexes were separated on 5%–10% polyacrylamide gradient gels. The CN-PAGE strips were cut and supercomplexes denatured. After 10 min incubation in equilibration buffer (urea 6 M TrisHCl pH8.8 1.5 M, SDS 2% glycerol 2%), the strips were incubated a second time in equilibration buffercontaining dithiotreitiol to reduce the disulfide bonds. The strips were

then incubated a third time in the same buffer containing iodoacetamide to avoid disulfide bond reformation. The lanes were incubated an extra 10 min in equilibration buffer before loading the lanes onto a 12% SDS-PAGE for separation in the second dimension. SDS-PAGE were electrotransferred into PVDF membranes, and immunodetection was carried out as described above.

***Electron microscopy***

Cells were fixed by incubation for 24 h in 4% paraformaldehyde, 1% glutaraldehyde in 0.1 M phosphate buffer (pH 7.2). Samples were then washed in phosphate-buffered saline (PBS) and post-fixed by incubation with 2% osmium tetroxide for 1 h. Samples were then fully dehydrated in a graded series of ethanol solutions followed by a propylene oxide bath. Pre-impregnation step was made by a propylene oxyde/Epon resin mixture (Sigma) and finally overnight in pure resin for impregnation of the samples. Cells were then embedded in Epon resin (Sigma), which was allowed to polymerize for 48 h at 60°C. Ultra-thin sections (90 nm) of these blocks were obtained with a Leica EM UC7 ultramicrotome (Wetzlar, Germany). Sections were deposited on gold grids and stained with 2% uranyl acetate, 5% lead citrate. Microscopy was performed using a JEOL 1011 transmission electron microscope. Images were analyzed using ImageJ software (NIH).

***Confocal microscopy***

HepaRG hepatocyte-like cells from DMSO treated cultures were cultivated for 24 h in Lab Tek slides. In order to stain mitochondrial network, cells were incubated with 0.5 µM MitoTracker Red CMX ROS (Invitrogen). The cells were washed with PBS, fixed with 4% paraformaldehyde solution. The slides were prepared using Prolong® Gold reagent with DAPI (Life Technologies) in order to stain nuclei. MitoTracker Red CMX ROS was excited at 543 nm, and fluorescence

emission was detected between 550 and 650 nm. 3D reconstruction was performed using Imaris software, permitting quantification of total volume of mitochondria, number of fragments per cell and fragment average volume.

***Statistical analysis***

Data were expressed as mean ± S.E.M. Statistical analyses were performed using GraphPad Prism®. Comparisons between human hepatoma cell lines to primary hepatocytes were performed using Kruskal-Wallis non parametric test followed by Dunns post test. The differences between shCTL and shCLS cells were evaluated by non parametric Wilcoxon matched-pairs signed rank test. Values showing $p<0.05$ were considered statistically significant unless otherwise indicated.

## Results

### *Validation of HepaRG cell line for mitochondrial bioenergetics studies.*

To study CL involvement in hepatic mitochondrial bioenergetics we investigated what would be the most appropriate human hepatocyte cell line to perform our experimentation. Primary cultured hepatocytes from human liver resection are rare and do not maintain a differentiated hepatocyte phenotype for extended periods of time post resection. Thus, we compared oxygen consumption in different energy states in three human differentiated hepatoma cell lines: HepG2, Huh7 and HepaRG to primary human hepatocytes cultured for 2 to 4 days following liver resection and hepatocyte isolation (figure 1A). In phosphorylating condition (state 3) oxygen consumption was significantly higher in HepaRG and primary human hepatocytes (125.4 and 144.8 pmol oxygen. $min^{-1}$ per $10^{-6}$ cells, respectively) than in Huh7 and HepG2 (41.8 and 54.8 pmol oxygen. $min^{-1}$ per $10^{-6}$ cells, respectively). Oxygen consumption in state 3 was similar between HepaRG and primary human hepatocytes cells. In non-phosphorylating condition (state 4), oxygen consumption of primary human hepatocytes was 4.6-, 3- and 1.4-fold higher than Huh7, HepG2 and HepaRG cells, respectively. Maximum oxygen consumption, reflecting maximal electron transport chain activity, measured in the presence of FCCP was significantly higher among HepaRG and human primary hepatocytes (156.7 and 176.7 pmol oxygen. $min^{-1}$ per$10^{-6}$ cells, respectively) than Huh7 and HepG2 (38.4 and 73.3 pmol oxygen. $min^{-1}$ per $10^{-6}$ cells, respectively). These results demonstrated that HepaRG hepatocyte-like cells exhibited similar oxygen consumption in different energy states when compared with primary human hepatocytes.

**Figure 1: HepaRG is the closest cellular model to mimic primary human hepatocyte mitochondrial bioenergetics and CL content.**

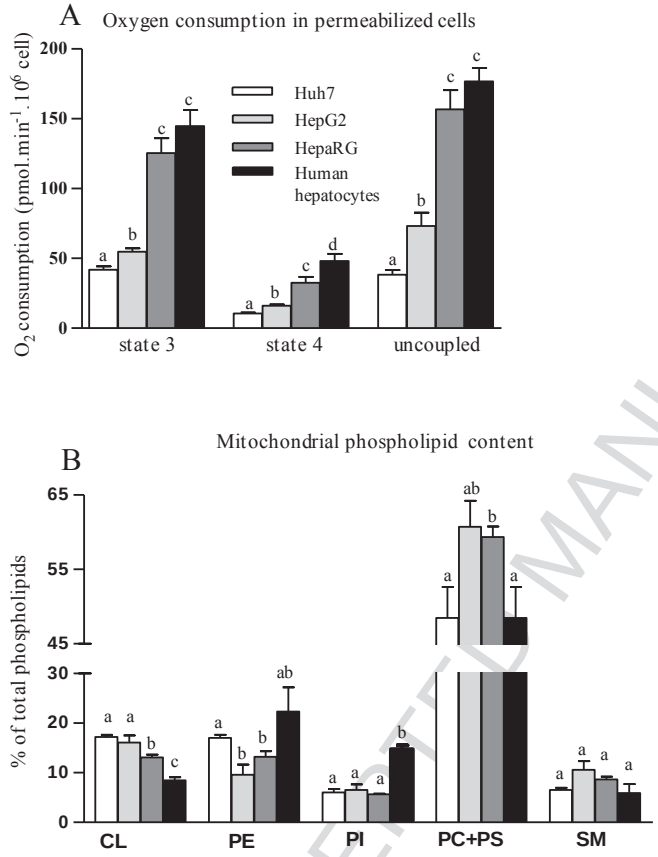


**Comparison of Huh7 (white bars), HepG2 (light grey bars) and HepaRG (dark grey bars) hepatocytes cell lines with primary human hepatocytes from liver resection (black bars).** *(A) oxygen consumption measured on permeabilized cells with pyruvate + malate + succinate as substrates, and (B) mitochondrial phospholipid classes content expressed in % of total mitochondrial phospholipids. Values represent the mean ± S.E.M. with N = 8 per group for Huh7, HepG2, HepaRG cells and N = 3 to 5 for primary human hepatocytes. Statistics: Different letters (a,b,c,d) for (A) each energy state and (B) each phospholipid class indicate significant difference ($p<0.05$). CL: cardiolipin, PE: phosphatidylethanolamine, PI: phosphatidylinositol, PC+PS: phosphatidylcholine + phosphatidylserine, SM: sphingomyelin.*

Mitochondrial phospholipid composition of the three cell lines was compared to primary human hepatocytes with a specific interest for CL (figure 1B). CL content was significantly lower in human hepatocytes (8.5% of total mitochondrial PL) than in Huh7 (17.2%), HepG2 (16.1%) and HepaRG (13.1%). PE content was not significantly different between human hepatocytes and the three hepatocytes cell lines. However Huh7 cells had significant higher PE content than HepG2 and HepaRG cells. Primary human hepatocytes had a significantly higher content in PI (14.8% of total mitochondrial PL) than the three cell lines (6%). PC + PS content was significantly lower (-9%) in Huh7 and (-9%) in primary human hepatocytes compared to HepaRG cell line. There were no significant differences in SM content between the hepatoma cell lines and the primary human hepatocytes (figure 1B). We chose to use the HepaRG cell line to generate CLS knockdown hepatocytes due to its similarity in mitochondrial bioenergetics and CL content.

***Characterization of shCLS recombinant HepaRG cells***

CLS mRNA was reduced 55% in shCLS compared to shCTL cells ($p = 0.014$, figure 2A). The reduction in gene expression was associated with a lower CLS protein expression in shCLS (40%, $p=0.028$, figure 2B) compared to shCTL. In addition, CL content was reduced in shCLS cells (45%, $p<0.05$) compared to shCTL (figure 2C). There was no difference in the content of other phospholipids. CL molecular species were analyzed by LC-MS/MS in shCLS and shCTL cells. Several differences in CL molecular species were observed (figure 2D). $(18:2)_3$-(16:1), which represents 15% of CL molecular species in shCTL cells, was reduced (-9%; $p=0.028$) in shCLS cells compared to shCTL. In addition, (16:1)-$(18:1)_2$-(18:2), which represents 5% of the molecular species in shCTL cells, was reduced by -21% ($p=0.028$) in shCLS cells compared to shCTL. Several modifications in less abundant (from 2% to 0.05%) CL molecular species content were observed in shCLS compared to shCTL.

**Figure 2: Characterization of cell line with shRNA targeting cardiolipin synthase.**

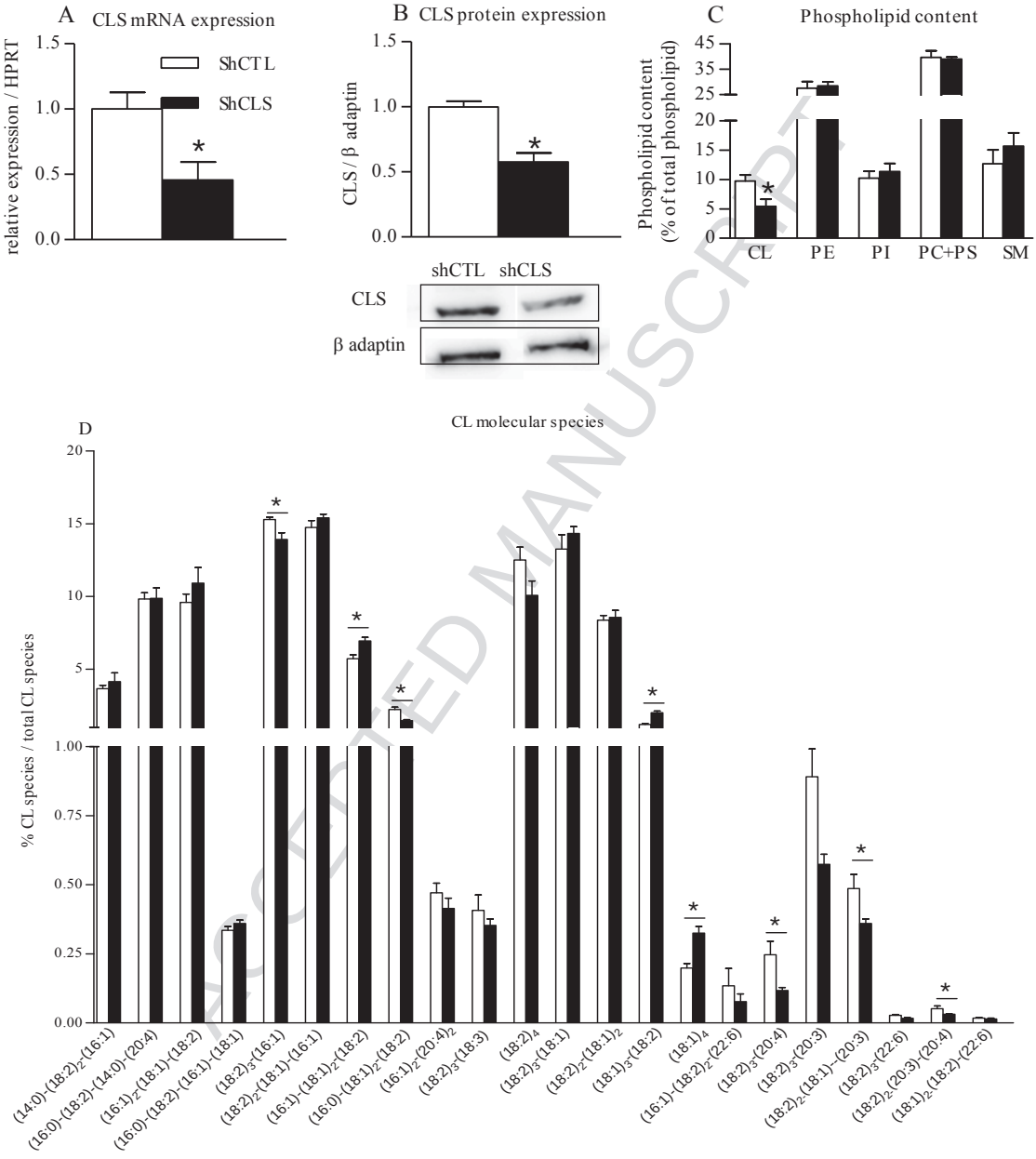


**ShCLS HepaRG cells characterization** *by (A) CLS mRNA expression, (B) CLS protein expression, (C) mitochondrial phospholipid content and (D) CL molecular species profile. Values represent the mean ± S.E.M. shCTL HepaRG cells (white bars) and shCLS HepaRG cells (black bars) with N = 6 per group. * = p<0.05.*

***Mitochondrial bioenergetics is altered in shCLS recombinant HepaRG cells***

We determined the effect of lowered CL on mitochondrial bioenergetics in HepaRG cells. The oxygen consumption measurements were performed on permeabilized cells in order to control the nature of the substrates and the respiratory complexes involved.

**Figure 3: Decrease in CL content affect overall respiratory chain function**

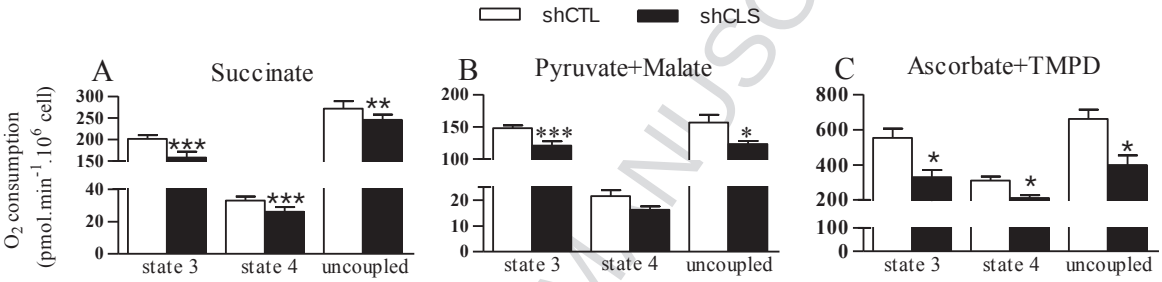


**Oxygen consumption measured on permeabilized cells** *using (A) succinate, (B) pyruvate + malate and (C), ascorbate + TMPD as substrates. Values represent the mean ± S.E.M. shCTL HepaRG cells (white bars) and shCLS HepaRG cells (black bars) with N = 6 per group. * = p<0.05, ** =p< 0.001 and *** = p<0.0001.*

In phosphorylating state (state 3), shCLS cells exhibited a significant decrease in oxygen consumption with all the substrates used compared to shCTL (26% with succinate, 21% with pyruvate+malate and 40% with ascorbate+TMPD) (figure 3A, B and C). In non-phosphorylating (state 4) oxygen consumption was significantly decreased by 33% (p=0.018) with succinate and 42% (p=0.018) with TMPD+ascorbate in shCLS cells (figure 3A and C). With pyruvate+malate oxygen consumption was unchanged (figure 3B and C). Finally, uncoupled state related-oxygen consumption was decreased in shCLS cells compared to shCTL cells (16% (p=0.015) with succinate, 23% (p=0.015) with pyruvate+malate and 40% (p=0.015) with ascorbate+TMPD.

***Mitochondrial respiratory supercomplexes organization is altered in shCLS recombinant HepaRG cells***

We examined mitochondrial respiratory supercomplexes organization in these cells. There was no difference in complex I, II, III and IV protein levels in shCLS cells compared to shCTL cells (figure 4A).

**Figure 4: Increased low molecular weight supercomplexes in cells with reduced CL content**

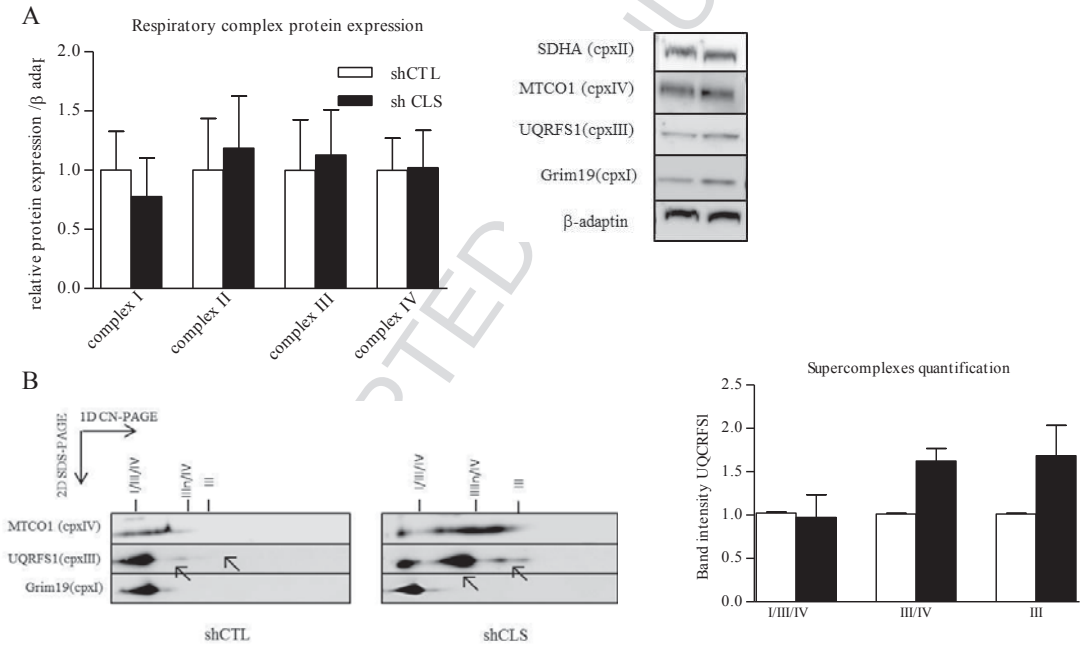


*(A) Respiratory complexes were quantified in ShCTL and ShCLS cells by densitometry after SDS-PAGE (N = 6 per group), (B) Digitonin-solubilized isolated mitochondria from shCTL and shCLS cells were analyzed by 2D CN/SDS-PAGE (N = 3 per group). Antibodies against Grim19, SDHA, UQRFS1, and MTCO1 were used to detect complexes I, II, III, and IV, respectively. Values represent the mean ± S.E.M. shCTL HepaRG cells (white bars) and shCLS HepaRG cells (black bars). Black arrows: highlighted modifications on complex III related supercomplexes.*

The supercomplexes composition was then investigated using two-dimensional electrophoresis with CN-PAGE followed by SDS-PAGE. In shCTL and shCLS cells supercomplexes were mainly composed of I/III/IV. However shCLS cells had higher content of low molecular supercomplexes such as III/IV and III than shCTL (figure 4B). Quantification of complex III band intensity revealed that III/IV and III were 60% higher in shCLS than in shCTL, without reaching statistical significance ($p=0.06$, figure 4B). In contrast, supercomplexes I/III/IV did not differ between shCLS and shCTL cells ($p=0.64$).

***Mitochondrial network is fragmented in shCLS recombinant HepaRG cells***

Mitochondrial network status, which is a balance between fusion and fission processes, can be modified by CL and can regulate mitochondrial bioenergetics [36]. Mitochondrial network was analyzed by confocal microscopy. Images obtained after 3-D reconstruction indicated that shCLS cells had a fragmented mitochondrial network compared to shCTL (figure 5A).

This difference was confirmed by several quantitative parameters. Total mitochondrial volume per cell was similar between shCTL and shCLS cells (figure 5B). In shCLS cells, mitochondrial network fragment number was 2.8-fold higher ($p<0.0001$) than in shCTL cells (figure 5C). Average volume of the fragments was 3-fold lower ($p<0.0001$) in shCLS cells than in shCTL cells (figure 5D). Protein expression of Drp1 a protein involved in fission and Mfn2 involved in fusion were quantified (figure 5E and F). A 35% increase in Drp1 protein expression in mitochondria was observed in shCLS compared to shCTL cells ($p= 0.042$). Mfn2 expression was similar between shCTL and shCLS cells.

**Figure 5: Decrease CL content induced mitochondrial network fragmentation**

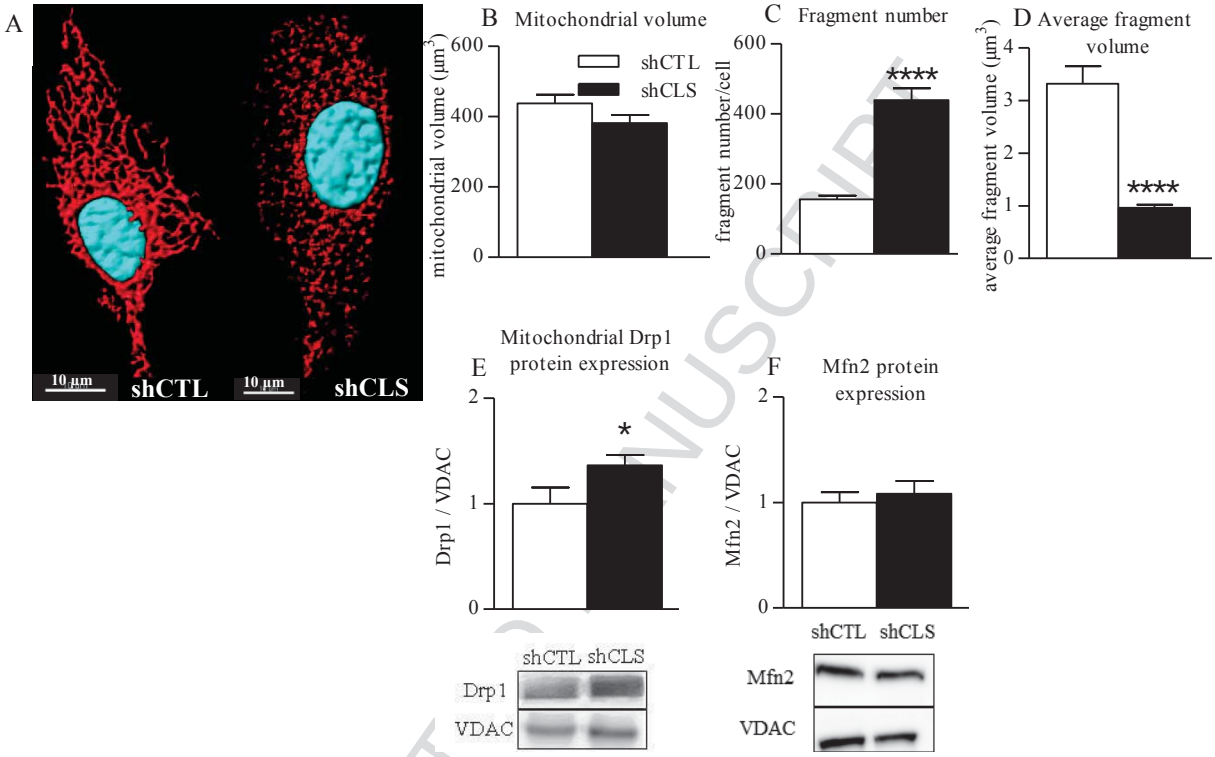


**Mitochondrial network analysis by confocal microscopy after mitotracker red staining**

*Three dimension reconstruction in shCTL (white bars) and shCLS (black bars) HepaRG cells was performed using Imaris software (nucleus in blue, and mitochondria in red). Representative mitochondrial network is shown in (A). Mitochondrial volume (B), mitochondrial fragment (C) and average fragment volume (D) were measured. Drp1 (E) and Mfn2 (D), proteins involved in fission and fusion were quantified by densitometry after SDS-PAGE. VDAC was used as loading control (N = 6). Values represent the mean ± S.E.M. * = p<0.05; **** = p<0.0001.*

***Reduced CL content increases ATP synthesis yield***

ATP synthesis rate was unaffected by a decrease in CL content in shCLS compared to shCTL cells (figure 6A). However ATP:O ratio reflecting ATP synthesis yield was significantly increased by 46% (p=0.0156) in shCLS cells compared to shCTL cells (figure 6B). ATP synthase protein expression was similar between shCLS and shCTL cells (figure 6C).

**Figure 6: Decrease in CL results in increased mitochondrial ATP synthesis efficiency without effects on ATP synthesis rate and ATP synthase protein**

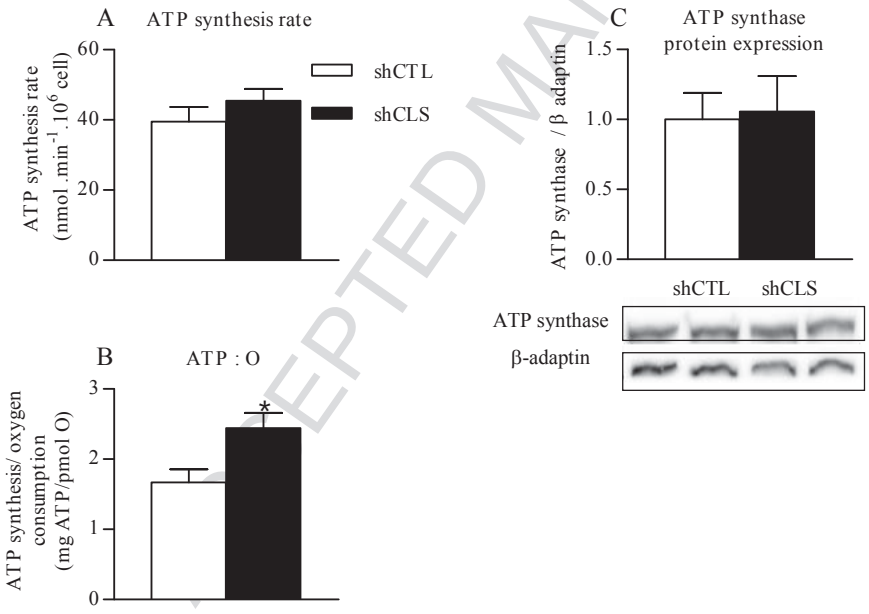


*(A) Mitochondrial ATP synthesis rate, (B) ATP synthesis efficiency expressed as the ratio of ATP synthesized and oxygen consumed were measured with succinate as substrate and (C) ATP synthase protein content with significant western blot tent. Values represent the mean ± S.E.M. shCTL HepaRG cells (white bars) and shCLS HepaRG cells (black bars) with N = 6 per group. * = p<0.05.*

***Decrease in CL content does not alter mitochondrial biogenesis or structure***.

A reduction in respiratory chain capacities can be compensated by an increase in mitochondrial biogenesis. Protein expression of mtTFA (figure 7A) and PGC-1α (figure 7B), involved in mitochondrial biogenesis, were unchanged between shCTL and shCLS cells.

**Figure 7: Decrease CL content did not affect mitochondrial biogenesis nor mitochondrial ultrastructure**

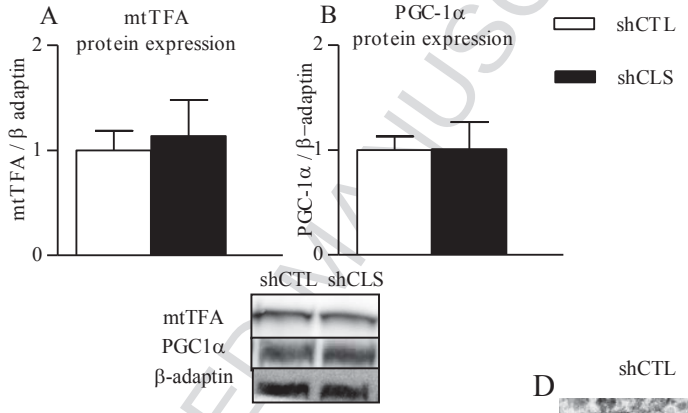


C

| | shCTL | shCLS | P value |
|---|---|---|---|
| Mitochondria number/cells | 160.8 ± 13.1 | 158.0 ± 16.6 | 0.3223 |
| Mitochondrial area (μm$^2$) | 19.96 ± 1.72 | 19.10 ± 1.67 | 0.5929 |
| Cristae total length (nm) | 1610 ± 207 | 1787 ± 239 | 0.6343 |
| Cristae length / OMM length | 0.518 ± 0.030 | 0.449 ± 0.025 | 0.1180 |

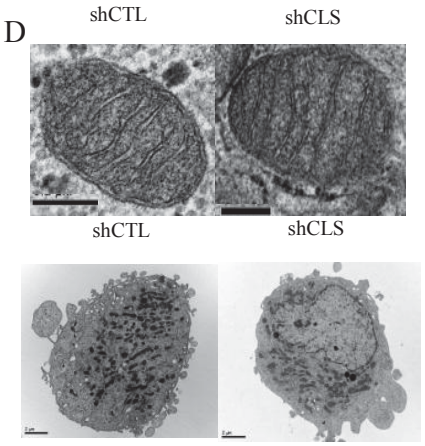


*Biogenesis protein marker (A) mtTFA and (B) PGC-1α were quantified by densitometry after western blotting. (C) Mitochondrial ultrastucture parameters and (D) Representative EM images of HepaRG cells and mitochondria from shCTL and shCLS cells. Bar is 2 μM for the lower panels and 0.2 μM for the upper panels. Values represent the mean ± S.E.M. shCTL HepaRG cells (white bars) and shCLS HepaRG cells (black bars) with N = 6 per group. OMM: outer mitochondrial membrane.*

Moreover, analyses of mitochondria area did not reveal any difference between shCLS and shCTL cells (figure 7C). This was confirmed by determination of mitochondrial number which

was similar between shCTL and shCLS cells (figure 7 C). As CL content can affect mitochondria ultrastructure [37], mitochondrial cristae and outer mitochondrial membrane (OMM) lengths were quantified. Neither cristae length nor cristae/OMM length ratio were altered by reduction in CL content in shCLS compared to shCTL cells (figure 7C and D).

**Discussion**

The overall aim of the present study was to investigate the involvement of CL content on mitochondrial bioenergetics in hepatocytes. We previously demonstrated that an increase in CL content in liver mitochondria led to a reduction in ATP synthesis yield. These data brought for the first time a direct causality between the increase in mitochondrial membrane CL content and reduction in efficiency of ATP synthesis [31]. In order to improve our understanding of the mechanisms related to mitochondrial bioenergetics modulation by CL, the effect of moderate decrease in CL content on mitochondrial bioenergetics in human hepatocytes were investigated.

We first compared three hepatoma cell lines to primary human hepatocytes, obtained from liver resection, in order to use the most relevant hepatic cellular model. Primary cultured hepatocytes from human liver resection are difficult to obtain. Moreover, primary human hepatocytes did not keep the hepatocyte phenotype for sufficient duration in order to perform our study. We chose to compare primary human hepatocytes to the most used human hepatocyte cell lines initially isolated from primary liver carcinomas: Huh7, HepG2 and HepaRG. Huh7 and HepG2 are commonly used as a model for liver cancer studies whereas the HepaRG cell line was defined as a new tool to study drug metabolism [38]. HepaRG appears to be an alternative to primary human hepatocytes because they retain a differentiated hepatocyte-like morphology and most liver functions, including cytochrome P450 drug-metabolizing and liver specific proteins such as aldolase, haptoglobulin and albumin [38]. However, to our knowledge there had been no analysis of HepaRG mitochondrial bioenergetics in comparison with primary human hepatocytes. Thus, we measured mitochondrial phospholipid content and oxygen consumption in different energy states with different substrates in permeabilized Huh7, HepG2, HepaRG and primary human hepatocytes. We observed that HepaRG mitochondrial oxygen consumption was closer to primary human hepatocytes than the two other cells lines at each respiratory state. Indeed both HepaRG and primary human hepatocytes exhibited significant oxidative phosphorylation

activity. In contrast, Huh7 and HepG2 cells had a much lower oxygen consumption. Under normal conditions, cells rely on mitochondrial oxidative phosphorylation to provide energy for cellular activities. Cancer cells are often characterized by increased “lactic” glycolysis and reduced mitochondrial respiratory function [39]. Here, the differentiated hepatocyte-like HepaRG cells appeared to have lost their cancer cell energy metabolism characteristics. Mitochondrial phospholipid composition was more heterogeneous between the different cell lines and primary human hepatocytes. However, HepaRG and primary human hepatocytes had a lower amount of CL than Huh7 and HepG2 cells. These data suggest that HepaRG may serve as a useful cell line for bioenergetics studies as an alternative to primary human hepatocytes.

In order to investigate the effect of reduction in CL content on mitochondrial function a recombinant HepaRG expressing shRNA for CLS was established. The decrease in CL content observed in shCLS HepaRG cells (-45%) was similar to that observed in primary rat neurons transfected with CLS RNAi [40] and in human lung carcinoma A549 cells transfected with shRNA encoding CLS [27]. The alteration in CL fatty acid composition observed in shCLS HepaRG cells indicated that reduction in CL content may alter CL remodeling processes. CL remodeling by MLCLAT 1 has previously been shown to be regulated in concert with CL content either in hyper or hypothyroid rat heart [41]. Furthermore, previous studies have reported acyl chain specificity for CLS. In fact, oleoyl and linoleyl species seem to be preferentially used as acyl donor by the CLS [42,43]. We can then speculate that in shCLS cells reduction in CLS was associated with changes in CL acylation. Changes in CL acylation mediated by CLS and in remodeling processes could be implied by the observed modifications in the CL fatty acid composition in shCLS cells. However, this fatty acid composition was still characteristic of mammalian mitochondria (major species are composed of linoleic acid 70 to 90% of CL fatty acid in rats[44]).

Reduction in CL content in shCLS HepaRG cells induced profound modifications in mitochondrial bioenergetics. Regardless of the substrate used and the energy state (non-phosphorylating, phosphorylating and uncoupled states) examined, oxygen consumption was significantly reduced from 16% to 41% suggesting a global decrease in respiratory chain activity. There are few studies in mammalian cells that have utilized RNAi to reduce CL content, and most of these have not considered mitochondrial bioenergetics [10,27,40]. Several studies in yeast have been focused on bioenergetics and CL content using Δcrd1 mutant yeast [1,21,22,45]. In these studies, reduced CL resulted inreduction in oxygen consumption in different energy states and resulted in mitochondrial uncoupling. In contrast, no alteration in oxygen consumption was observed in intact Barth syndrome fibroblasts which exhibit reduced CL levels [28]. However a reduction in oxygen consumption in phosphorylating and in uncoupled states in isolated mitochondria from Barth syndrome fibroblast indicated a compensatory increase in mitochondrial mass/cell [28]. A strong reduction in oxygen consumption was observed in induced pluripotent stem cells derived from Barth syndrome patients [29]. Comparison of our data with these studies should be considered with caution since Barth syndrome is characterized by not only a lower CL content but an increase in MLCL content [37]. A CHO cell line containing a temperature-sensitive mutant of PG synthase provided the first indication of the potential involvement of CL in mammalian mitochondrial bioenergetic [25]. At the non-permissive temperature (40°C) mutant CHO cells exhibited a decrease in oxygen consumption and ATP production. However, since PG synthase mutation induced a reduction in both PG and CL content, it is not possible to attribute the mitochondrial bioenergetics defects to CL alone. More recently, in alpha-synuclein knockout mice a 22% reduction in CL content in brain was associated with a 15% reduction in complex I/III activity without changes in individual complexes activities [26]. In addition, PTPMT1 KO mice and cells exhibited a 3.5-fold reduction in CL content associated with a large decrease in oxygen consumption [20]. Our results on

impairment of mitochondrial respiratory chain activity in shCLS HepaRG cells are in agreement with these studies.

We investigated the mechanisms potentially responsible for the observed reduction in respiratory chain function in shCLS cells.

Organization of respiratory complexes into supercomplexes facilitates electron transfer through oxidative phosphorylation (OXPHOS) and leads to a better functioning of the mitochondrial respiratory chain [46]. Since CL may be required for supercomplexes stability [2,3,47,48], reduction in CL content in shCLS HepaRG cells could potentially affect supercomplexes and consequently OXPHOS. A lower amount of supercomplexes organization with a higher content in low molecular supercomplexes such as III/IV and III were observed when CL content was reduced in shCLS cells. These defects could explain the overall decrease in respiratory chain activity. Supercomplexes destabilization have been observed in cells from a Barth syndrome patient [28]. However, as indicated above the supercomplexes alteration may have been due to reduction in CL and/ or an increase in MLCL. A recent study in an αTFP knock out mouse model did not demonstrated alteration in supercomplexes organization in liver [49]. This difference could be due to a lower reduction in CL content (-20%) in the αTFP knock out mouse compared to shCLS HepaRG cells used in the present study (-45%).

Alteration in mitochondrial network by reduction in CL content in shCLS cells was explored using confocal microscopy. shCLS cells had a largely fragmented mitochondrial network in comparison to shCTL cells. Dissipation of the mitochondrial membrane potential using pharmacologic agents such as FCCP have been shown to induce mitochondrial network fragmentation [50,51]. Moreover, a fragmented mitochondrial network was observed when CL content was reduced in *Saccharomyces cerevisiae* [52]. However, the mechanisms that explain how disrupted CL content could affect mitochondrial dynamics are not well understood. Using *In silico* analysis, it was reported that CL can mediate DRP1 fixation into the liposome and

stimulate the GTPase activity of DRP1 [4,53]. In the present study, DRP1 protein expression in mitochondria of shCLS was increased without a modulation in Mfn2 expression. To our knowledge this is the first study reporting mitochondrial network modulation by reduced CL content in mammals. The present results are in agreement with those of Joshi *et al*. obtained in yeast [52]. However, increase DRP1 recruitment to mitochondria with lower CL content is not intuitive since DRP1 oligomerization and GTPase activity require CL. As suggested by Joshi *et al.*, CL content reduction could affect fusion related protein and disturb fission/fusion balance [52]. Elucidation of this specific point will need further investigation.

In the present study, increased fission without opposed fusion has the potential to result in fragmentation of the mitochondrial network in shCLS cells. Fragmented mitochondrial network in shCLS cells could explain, in part, the decrease in respiratory chain activity induced by CL loss.

Since oxidation and phosphorylation are coupled a decrease in oxygen consumption can affect ATP synthesis. The ATP synthesis rate was similar between shCTL and shCLS cells. In the same way ATP synthase expression was unchanged in shCTL compared to shCLS cells. Thus, ATP synthesis was not maintained by an increase in ATP synthase protein expression. Results obtained in other models of decreased CL content are contradictory. Human lung carcinoma A549 cells transfected with shRNA targeting CLS had a 60% reduction in the total cellular ATP level [27]. However, it is important to point out that mitochondrial ATP production was not measured, which is a central parameter in cancer cells using lactic glycolysis for ATP supply. On the contrary, lymphoblasts generated from Barth syndrome patients did not exhibit modification of ATP content or ATP synthesis rate despite decreased oxygen consumption [28]. Despite decreased mitochondrial membrane potential, mitochondrial ATP synthesis was enhanced in lymphoblasts from Barth syndrome patients compared to control subjects. Increased

mitochondrial biogenesis has been found to be a compensatory mechanism for OXPHOS dysfunction in Barth syndrome [28] [54]. However, in the present study we did not observe an increase in mitochondrial mass and the mitochondrial biogenesis protein markers PGC1α and mtTFA. Thus, mitochondrial biogenesis could not explain how mitochondrial ATP synthesis rate was maintained in shCLS HepaRG cells. Moreover, we explored mitochondrial cristae since several studies suggested a role of CL in cristae ultrastructure [55–57]. We did not observe modification of the mitochondrial cristae ultrastructure, contrary to data reported in yeast [58]. However alteration in cristae morphology has not be consistently observed in Δ TAZ yeast [59]. Defects of mitochondrial organization could lead to ATP synthesis disturbances as ATP synthase is localized in the cristae and participates in increasing the efficiency of OXPHOS, ensuring proximity between ANT and ATP synthase. We examined ATP synthesis rate to oxygen consumption (ATP:O ratio) which is reflective of ATP synthesis yield. ATP:O ratio was significantly increased by 46% in shCLS compared to shCTL cells indicating that shCLS cells were more efficient in ATP synthesis. This is in agreement with data reported in liver mitochondria from hypothyroid rats, where oxygen consumption is reduced [60] associated to lower CL content [61] and higher ATP synthesis efficiency [60]. However, the present data are not in agreement with yeast and that observed in Barth syndrome cells. CLS null yeast, as explained in the introduction, exhibit several bioenergetics differences in the respiratory chain, moreover the effect of total absence of CL compared to a moderate decrease in CL content can be entirely different. Barth syndrome is defined by an increase in the MLCL/CL ratio. Indeed, most of the effects of TAZ mutation are due to the increase in MLCL content in mitochondria. Moreover most data published on Barth syndrome utilize cells with a low metabolic activity (leucocyte, lymphoblast, mouse embryonic fibroblast). This may explain the differences observed between these cells and the results reported in the present study. A recent publication in immortalized lymphoblasts from Barth syndrome patients suggested an increase in mitochondrial

content as a mechanism to compensate for reduction in respiratory chain activity [28]. This is a good illustration of the variability in mitochondrial adaptation mechanisms to respiratory chain reduced activity. Finally, Zhang *et al*. using PTPMT1 KO mice, showed that reduction in CL content and respiratory chain was associated with an increase in glycolysis to compensate for lower mitochondrial activity [20]. The present study was performed in the HepaRG hepatocyte cell line, which exhibit a high content in mitochondria indicating highly metabolic activity which is much different from mouse embryonic fibroblasts. It seems apparent that reduction in oxidative capacities in mouse embryonic fibroblast cannot be compensated by an increase in ATP synthesis efficiency, but by glycolysis.

Interestingly, in our previous work on liver mitochondria an increase in CL content resulted in the exact opposite effect, a reduction in ATP synthesis yield [31]. These two experimental models clearly demonstrated a direct regulation of ATP synthesis yield by CL content.

In conclusion, the present study makes important advancements in our understanding of the role of CL in human cell mitochondrial bioenergetics. A moderate reduction in CL content in shCLS cells resulted in lowered respiratory chain activity that could be due to both supercomplexes destabilization and mitochondrial network fragmentation. The reduction in mitochondrial oxidative capacities in shCLS cells was not associated with lower ATP synthesis but induced an increase in ATP synthesis yield. Compensatory mechanism leading to maintained ATP synthesis rate needs to be further investigated. The present study, with our previous published data, demonstrate that the cellular CL content is part of the regulation in mitochondrial ATP synthesis yield.

**Acknowledgements**

This paper is dedicated to the memory of William A. Taylor who passed away prematurely during this study. Authors thanks Julien Gaillard from « Plateforme R.I.O. de Microscopie Electronique de l'Université François Rabelais de Tours » for his precious technical support, and Jean Paul Lasserre (I.B.G.C – UMR5095 CNRS/Université de Bordeaux, team Molecular Genetics of Mitochondrial Systems) for the CN-Page training of Laure Peyta. This work was funded by "Ligue contre le Cancer" (16, 18, 37, 72 and 85 committees), Région Centre (LIPIDS project of ARD2020-Biomedicaments), "Cancéropole Grand Ouest", "Groupe Lipides Nutrition" and "Association CANCEN". Laure Peyta received a fellowship from"Ministère de l'Enseignement Supérieur et de la Recherche ». This work was supported by grants from the CIHR (MOP-106428) and Heart and Stroke Foundation of Canada (G.M.H. G-14-0005708). G.M.H. is a Canada Research Chair in Molecular Cardiolipin Metabolism.

**References**


1. Zhong Q, Gohil VM, Ma L, Greenberg ML. Absence of cardiolipin results in temperature sensitivity, respiratory defects, and mitochondrial DNA instability independent of pet56. J Biol Chem. 2004;279: 32294–300. doi:10.1074/jbc.M403275200
2. Zhang M, Mileykovskaya E, Dowhan W. Cardiolipin is essential for organization of complexes III and IV into a supercomplex in intact yeast mitochondria. J Biol Chem. 2005;280: 29403–8. doi:10.1074/jbc.M504955200
3. Bazán S, Mileykovskaya E, Mallampalli VKPS, Heacock P, Sparagna GC, Dowhan W. Cardiolipin-dependent reconstitution of respiratory supercomplexes from purified Saccharomyces cerevisiae complexes III and IV. J Biol Chem. 2013;288: 401–11. doi:10.1074/jbc.M112.425876
4. Bustillo-Zabalbeitia I, Montessuit S, Raemy E, Basañez G, Terrones O, Martinou J-C. Specific interaction with cardiolipin triggers functional activation of Dynamin-Related Protein 1. Strack S, editor. PLoS One. Public Library of Science; 2014;9: e102738. doi:10.1371/journal.pone.0102738
5. Gebert N, Joshi AS, Kutik S, Becker T, McKenzie M, Guan XL, et al. Mitochondrial cardiolipin involved in outer-membrane protein biogenesis: implications for Barth syndrome. Curr Biol. Elsevier Ltd; 2009;19: 2133–9. doi:10.1016/j.cub.2009.10.074
6. Gaspard GJ, McMaster CR. The mitochondrial quality control protein Yme1 is necessary to prevent defective mitophagy in a yeast model of Barth syndrome. J Biol Chem. 2015;290: 9284–98. doi:10.1074/jbc.M115.641878
7. Hsu P, Liu X, Zhang J, Wang H-G, Ye J-M, Shi Y. Cardiolipin remodeling by TAZ/tafazzin is selectively required for the initiation of mitophagy. Autophagy. 2015;11: 643–52. doi:10.1080/15548627.2015.1023984
8. Wang L, Liu X, Nie J, Zhang J, Kimball SR, Zhang H, et al. ALCAT1 controls mitochondrial etiology of fatty liver diseases, linking defective mitophagy to steatosis. Hepatology. 2015;61: 486–96. doi:10.1002/hep.27420
9. Huang Z, Jiang J, Tyurin VA, Zhao Q, Mnuskin A, Ren J, et al. Cardiolipin deficiency leads to decreased cardiolipin peroxidation and increased resistance of cells to apoptosis. Free Radic Biol Med. 2008;44: 1935–1944. doi:10.1016/j.freeradbiomed.2008.02.016.Cardiolipin
10. Choi S-Y, Gonzalvez F, Jenkins GM, Slomianny C, Chretien D, Arnoult D, et al. Cardiolipin deficiency releases cytochrome c from the inner mitochondrial membrane and accelerates stimuli-elicited apoptosis. Cell Death Differ. 2007;14: 597–606. doi:10.1038/sj.cdd.4402020
11. Fry M, Green DE. Cardiolipin requirement for electron transfer in complex I and III of the mitochondrial respiratory chain. J Biol Chem. 1981;256: 1874–80.
12. Sharpley MS, Shannon RJ, Draghi F, Hirst J. Interactions between phospholipids and NADH:ubiquinone oxidoreductase (complex I) from bovine mitochondria. Biochemistry. 2006;45: 241–8. doi:10.1021/bi051809x
13. Paradies G, Petrosillo G, Pistolese M, Ruggiero FM. Reactive oxygen species affect mitochondrial electron transport complex I activity through oxidative cardiolipin damage. Gene. 2002;286: 135–41.

14. Schwall CT, Greenwood VL, Alder NN. The stability and activity of respiratory Complex II is cardiolipin-dependent. Biochim Biophys Acta. 2012;1817: 1588–96. doi:10.1016/j.bbabio.2012.04.015

15. Gomez B Jr RN. Phospholipase digestion of bound cardiolipin reversibly inactivates bovine cytochrome bc1. Biochemistry. 1999;38: 9031–8. doi:10.1021/bi990603r

16. Hunte C. Specific protein-lipid interactions in membrane proteins. Biochem Soc Trans. 2005;33: 938–42. doi:10.1042/BST20050938

17. Robinson NC. Specificity and binding affinity of phospholipids to the high-affinity cardiolipin sites of beef heart cytochrome c oxidase. Biochemistry. 1982;21: 184–8.

18. Robinson NC. Functional binding of cardiolipin to cytochrome c oxidase. J Bioenerg Biomembr. 1993;25: 153–63.

19. Sedlák E, Robinson NC. Phospholipase A(2) digestion of cardiolipin bound to bovine cytochrome c oxidase alters both activity and quaternary structure. Biochemistry. 1999;38: 14966–72.

20. Zhang J, Guan Z, Murphy AN, Wiley SE, Perkins GA, Worby C a, et al. Mitochondrial phosphatase PTPMT1 is essential for cardiolipin biosynthesis. Cell Metab. Elsevier Inc.; 2011;13: 690–700. doi:10.1016/j.cmet.2011.04.007

21. Jiang F, Ryan MT, Schlame M, Zhao M, Gu Z, Klingenberg M, et al. Absence of cardiolipin in the crd1 null mutant results in decreased mitochondrial membrane potential and reduced mitochondrial function. J Biol Chem. 2000;275: 22387–94. doi:10.1074/jbc.M909868199

22. Koshkin V, Greenberg ML. Oxidative phosphorylation in cardiolipin-lacking yeast mitochondria. Biochem J. 2000;347 Pt 3: 687–91.

23. Potting C, Wilmes C, Engmann T, Osman C, Langer T. Regulation of mitochondrial phospholipids by Ups1/PRELI-like proteins depends on proteolysis and Mdm35. EMBO J. Nature Publishing Group; 2010;29: 2888–98. doi:10.1038/emboj.2010.169

24. Baile MG, Lu Y-W, Claypool SM. The topology and regulation of cardiolipin biosynthesis and remodeling in yeast. Chem Phys Lipids. 2014;179: 25–31. doi:10.1016/j.chemphyslip.2013.10.008

25. Ohtsuka T, Nishijima M, Suzuki K, Akamatsu Y. Mitochondrial dysfunction of a cultured Chinese hamster ovary cell mutant deficient in cardiolipin. J Biol Chem. 1993;268: 22914–9.

26. Ellis CE, Murphy EJ, Mitchell DC, Golovko MY, Scaglia F, Barceló-Coblijn GC, et al. Mitochondrial lipid abnormality and electron transport chain impairment in mice lacking alpha-synuclein. Mol Cell Biol. 2005;25: 10190–201. doi:10.1128/MCB.25.22.10190-10201.2005

27. Chen B, Coon T a., Glasser JR, Zou C, Ellis B, Das T, et al. E3 Ligase Subunit Fbxo15 and PINK1 Kinase Regulate Cardiolipin Synthase 1 Stability and Mitochondrial Function in Pneumonia. Cell Rep. 2014;7: 476–487. doi:10.1016/j.celrep.2014.02.048

28. Gonzalvez F, D'Aurelio M, Boutant M, Moustapha A, Puech J-P, Landes T, et al. Barth syndrome: cellular compensation of mitochondrial dysfunction and apoptosis inhibition due to changes in cardiolipin remodeling linked to tafazzin (TAZ) gene mutation. Biochim Biophys Acta. Elsevier B.V.; 2013;1832: 1194–206. doi:10.1016/j.bbadis.2013.03.005

29. Dudek J, Cheng I-F, Balleininger M, Vaz FM, Streckfuss-Bömeke K, Hübscher D, et al. Cardiolipin deficiency affects respiratory chain function and organization in an induced pluripotent stem cell model of Barth syndrome. Stem Cell Res. 2013;11: 806–19. doi:10.1016/j.scr.2013.05.005

30. Bobyleva V, Bellei M, Pazienza TL, Muscatello U. Effect of cardiolipin on functional properties of isolated rat liver mitochondria. Biochem Mol Biol Int. 1997;41: 469–480.

31. Julienne CM, Tardieu M, Chevalier S, Pinault M, Bougnoux P, Labarthe F, et al. Cardiolipin content is involved in liver mitochondrial energy wasting associated with cancer-induced cachexia without the involvement of adenine nucleotide translocase. Biochim Biophys Acta. 2014;1842: 726–33. doi:10.1016/j.bbadis.2014.02.003

32. Gripon P, Rumin S, Urban S, Le Seyec J, Glaise D, Cannie I, et al. Infection of a human hepatoma cell line by hepatitis B virus. Proc Natl Acad Sci U S A. 2002;99: 15655–60. doi:10.1073/pnas.232137699

33. Bligh EG, Dyer WJ. A rapid method of total lipid extraction and purification. Can J Biochem Physiol. 1959;37: 911–7.

34. Folch J, Lees M, Sloane Stanley GH. A simple method for the isolation and purification of total lipides from animal tissues. J Biol Chem. 1957;226: 497–509.

35. Vial G, Chauvin M-A, Bendridi N, Durand A, Meugnier E, Madec A-M, et al. Imeglimin Normalizes Glucose Tolerance and Insulin Sensitivity and Improves Mitochondrial Function in Liver of a High-Fat High-Sucrose Diet Mice Model. Diabetes. 2014; doi:10.2337/db14-1220

36. Gomes LC, Di Benedetto G, Scorrano L. During autophagy mitochondria elongate, are spared from degradation and sustain cell viability. Nat Cell Biol. 2011;13: 589–98. doi:10.1038/ncb2220

37. Lu Y-W, Claypool SM. Disorders of phospholipid metabolism: an emerging class of mitochondrial disease due to defects in nuclear genes. Front Genet. 2015;6: 3. doi:10.3389/fgene.2015.00003

38. Guillouzo A, Corlu A, Aninat C, Glaise D, Morel F, Guguen-Guillouzo C. The human hepatoma HepaRG cells: a highly differentiated model for studies of liver metabolism and toxicity of xenobiotics. Chem Biol Interact. 2007;168: 66–73. doi:10.1016/j.cbi.2006.12.003

39. Wallace DC. Mitochondria and cancer. Nat Rev Cancer. 2012;12: 685–98. doi:10.1038/nrc3365

40. Ji J, Kline AE, Amoscato A, Arias AS, Sparvero LJ, Tyurin V a, et al. Lipidomics identifies cardiolipin oxidation as a mitochondrial target for redox therapy of brain injury. Nat Neurosci. 2012; doi:10.1038/nn.3195

41. Taylor WA, Xu FY, Ma BJ, Mutter TC, Dolinsky VW, Hatch GM. Expression of monolysocardiolipin acyltransferase activity is regulated in concert with the level of cardiolipin and cardiolipin biosynthesis in the mammalian heart. BMC Biochem. 2002;3: 9. doi:10.1186/1471-2091-3-9

42. Houtkooper RH, Akbari H, van Lenthe H, Kulik W, Wanders RJA, Frentzen M, et al. Identification and characterization of human cardiolipin synthase. FEBS Lett. 2006;580: 3059–3064. doi:10.1016/j.febslet.2006.04.054

43. Nie J, Hao X, Chen D, Han X, Chang Z, Shi Y. A novel function of the human CLS1 in

phosphatidylglycerol synthesis and remodeling. Biochim Biophys Acta. 2010;1801: 438–45. doi:10.1016/j.bbalip.2009.12.002

44. Wahjudi PN, K Yee J, Martinez SR, Zhang J, Teitell M, Nikolaenko L, et al. Turnover of nonessential fatty acids in cardiolipin from the rat heart. J Lipid Res. 2011;52: 2226–33. doi:10.1194/jlr.M015966

45. Jiang F, Rizavi HS, Greenberg ML. Cardiolipin is not essential for the growth of Saccharomyces cerevisiae on fermentable or non-fermentable carbon sources. Mol Microbiol. 1997;26: 481–91.

46. Schägger H. Respiratory chain supercomplexes. IUBMB Life. 2001;52: 119–28. doi:10.1080/15216540152845911

47. Pfeiffer K, Gohil V, Stuart RA, Hunte C, Brandt U, Greenberg ML, et al. Cardiolipin stabilizes respiratory chain supercomplexes. J Biol Chem. 2003;278: 52873–80. doi:10.1074/jbc.M308366200

48. Mileykovskaya E, Dowhan W. Cardiolipin-dependent formation of mitochondrial respiratory supercomplexes. Chem Phys Lipids. 2014;179: 42–8. doi:10.1016/j.chemphyslip.2013.10.012

49. Mejia EM, Ibdah JA, Sparagna GC, Hatch GM. Differential reduction in cardiac and liver monolysocardiolipin acyl transferase-1 and reduction in tetralinoleoyl-cardiolipin in the alpha subunit of trifunctional protein heterozygous knockout mice. Biochem J. 2015; doi:10.1042/BJ20150648

50. Ishihara N, Jofuku A, Eura Y, Mihara K. Regulation of mitochondrial morphology by membrane potential, and DRP1-dependent division and FZO1-dependent fusion reaction in mammalian cells. Biochem Biophys Res Commun. 2003;301: 891–898. doi:10.1016/S0006-291X(03)00050-0

51. Legros F, Lombès A, Frachon P, Rojo M. Mitochondrial Fusion in Human Cells Is Efficient, Requires the Inner Membrane Potential, and Is Mediated by Mitofusins. Mol Biol Cell . 2002;13 : 4343–4354. doi:10.1091/mbc.E02-06-0330

52. Joshi AS, Thompson MN, Fei N, Hüttemann M, Greenberg ML. Cardiolipin and mitochondrial phosphatidylethanolamine have overlapping functions in mitochondrial fusion in Saccharomyces cerevisiae. J Biol Chem. 2012;287: 17589–97. doi:10.1074/jbc.M111.330167

53. Ugarte-Uribe B, Müller H-M, Otsuki M, Nickel W, García-Sáez AJ. Dynamin-related Protein 1 (Drp1) Promotes Structural Intermediates of Membrane Division. J Biol Chem . 2014;289 : 30645–30656. doi:10.1074/jbc.M114.575779

54. Xu Y, Sutachan JJ, Plesken H, Kelley RI, Schlame M. Characterization of lymphoblast mitochondria from patients with Barth syndrome. Lab Invest. 2005;85: 823–830. doi:10.1038/labinvest.3700290

55. Acehan D, Xu Y, Stokes DL, Schlame M. Comparison of lymphoblast mitochondria from normal subjects and patients with Barth syndrome using electron microscopic tomography. Lab Invest. 2007;87: 40–8. doi:10.1038/labinvest.3700480

56. Schlame M, Ren M. The role of cardiolipin in the structural organization of mitochondrial membranes. Biochim Biophys Acta. 2009;1788: 2080–2083.

57. Acehan D, Malhotra A, Xu Y, Ren M, Stokes DL, Schlame M. Cardiolipin affects the supramolecular organization of ATP synthase in mitochondria. Biophys J. Biophysical

Society; 2011;100: 2184–2192. doi:10.1016/j.bpj.2011.03.031

58. Claypool SM, Boontheung P, McCaffery JM, Loo JA, Koehler CM. The cardiolipin transacylase, tafazzin, associates with two distinct respiratory components providing insight into Barth syndrome. Mol Biol Cell. 2008;19: 5143–55. doi:10.1091/mbc.E08-09-0896

59. Baile MG, Sathappa M, Lu Y-W, Pryce E, Whited K, McCaffery JM, et al. Unremodeled and remodeled cardiolipin are functionally indistinguishable in yeast. J Biol Chem. 2014;289: 1768–78. doi:10.1074/jbc.M113.525733

60. Nogueira V, Walter L, Avéret N, Fontaine E, Rigoulet M, Leverve XM. Thyroid status is a key regulator of both flux and efficiency of oxidative phosphorylation in rat hepatocytes. J Bioenerg Biomembr. 2002;34: 55–66.

61. Paradies G, Ruggiero FM, Dinoi P. The influence of hypothyroidism on the transport of phosphate and on the lipid composition in rat-liver mitochondria. Biochim Biophys Acta. 1991;1070: 180–6.